

## Level shifts of *msns* Rydberg states induced by hyperfine interaction in odd alkaline-earth isotopes

R. Beigang and A. Timmermann

*Institut für Atom- und Festkörperphysik, Freie Universität Berlin, 1000 Berlin 33, West Germany*

(Received 10 September 1981)

High-resolution two-photon spectroscopy was applied to investigate the *msns*  $^1S_0$  Rydberg states of the alkaline-earth elements Ca, Sr, and Ba. It is shown for  $^{43}\text{Ca}$ ,  $^{87}\text{Sr}$ ,  $^{135}\text{Ba}$ , and  $^{137}\text{Ba}$  that the hyperfine interaction causes a level shift between odd- and even-mass isotopes. A theoretical interpretation is presented which relates the energy-level shift for odd isotopes to the singlet-triplet separation which in turn is a function of the principal quantum number, and good agreement with the experimental results is found.

### I. INTRODUCTION

The important role of hyperfine-induced singlet-triplet mixing in two-electron systems has been demonstrated recently in the case of  $^3\text{He}$ .<sup>1</sup> The hyperfine interaction of the  $1s$  open-shell electron gives rise to a significant modification of the hyperfine structure of the  $n^3D$  states. The hyperfine structure was measured for the  $2^3P$  and  $3^3D$  states using intermodulated fluorescence spectroscopy<sup>1</sup> and for the  $n^3S$  ( $n=4-6$ ) and  $n^3D$  ( $n=3-6$ ) levels via Doppler-free two-photon spectroscopy.<sup>2</sup> In addition, the isotope shifts between  $^3\text{He}$  and  $^4\text{He}$  were then determined in these transitions.<sup>3,4</sup> The knowledge of the hyperfine structure is necessary to obtain accurate values for the isotope shifts. Liao<sup>1</sup> also pointed out that hyperfine-induced singlet-triplet mixing was of critical importance, in particular, for the character of high Rydberg states in two-electron systems.

The drastic influence of singlet-triplet mixing on the hyperfine structure of  $5snd^1D_2$  state of  $^{87}\text{Sr}$ , e.g., was reported recently, demonstrating that the hyperfine structure was a very sensitive probe for testing admixtures of other states.<sup>5</sup> Hyperfine-induced singlet-triplet mixing was responsible for an energy shift first observed for  $5sns^1S_0$  states of  $^{87}\text{Sr}$  for very high quantum numbers.<sup>6</sup> It was expected that this shift was typical of all two-electron systems with a magnitude proportional to the nuclear spin. In this paper we present experimental results on the level shifts induced by hyperfine interaction of *msns*  $^1S_0$  states of Ca, Sr, and Ba. These data clearly confirm the expected

behavior. Calculations of the level shifts for all alkaline-earth elements are in excellent agreement with the experimental data.

### II. EXPERIMENTAL

In order to overcome the Doppler broadening and to achieve high resolution, a Doppler-free experimental setup was used in combination with a narrow-band cw dye laser. The high resolution is necessary as the separation between different isotopes and hyperfine components is of the order of 10 to 500 MHz. Two-photon spectroscopy is particularly well suited for the investigations of high Rydberg states in Ca, Sr, and Ba, since the energy difference between the ground state and the *msns*  $^1S_0$  states can be bridged by two photons of an energy accessible with cw dye lasers. The output power necessary for two-photon transitions is obtainable with ring laser systems. These laser systems are ideal tools especially for high-resolution two-photon spectroscopy due to the high single-mode output power and narrow bandwidth.

The measurements reported here were carried out with a commercial ring dye laser (Spectra Physics 380) in the wavelength region between 406 and 480 nm, which was covered by three different dyes. For the spectroscopy of Ca, Sr, and Ba, Stilbene 1, Stilbene 3, and Coumarine 102 were used, respectively. All these dyes were pumped with the uv lines of an  $\text{Ar}^+$  ion laser providing a maximum pump power of 3.6 W. The most efficient of these dyes is Stilbene 3 with a tuning range of 420 nm to 470 nm, allowing for output powers up to 250 mW. Stilbene 1 working in the deep blue range be-

tween 405 nm to 425 nm resulted in a peak power of about 140 mW and Coumarine 102, providing wavelengths from 460 nm to 495 nm, yielded about 200 mW with the uv pump lines.

The dye laser was frequency stabilized to an external Fabry-Perot reference cavity resulting in a linewidth of about 1 MHz. The total continuous single-mode tuning range extended over 30 GHz, more than sufficient to measure all hyperfine components and isotopes of one Rydberg state in a single scan.

Doppler-free signals were obtained by applying the usual geometry for high-resolution two-photon spectroscopy<sup>7</sup> as sketched in Fig. 1. The metal vapor was produced in a stainless steel hot pipe heated to a temperature which corresponded to a vapor pressure of approximately 25 mTorr. To obtain the power density necessary for the two-photon process the laser beam was focused into the center of the pipe and reflected back via a spherical mirror. The excited Rydberg atoms were then detected by a space-charge limited thermionic diode with substantial gain for detection of ionization.<sup>8</sup> The diode was formed by a stainless steel wire inserted into the hot pipe and negatively biased ( $-0.5$  V) through a load resistor (10 to 100 k $\Omega$ ). This detection method is, in particular, well suited for the spectroscopy of high Rydberg states, because the sensitivity of the thermionic diode increases with

decreasing energy difference to the ionization limit. Thus it partly compensates for the decreasing transition probability.

The laser wavelength was determined by using a wave meter with an absolute accuracy of 0.01  $\text{cm}^{-1}$ . This accuracy is important to identify unambiguously the exact term energies and hence the quantum number  $n$  of the excited Rydberg state, especially in the range of high principal quantum numbers. Relative frequency separations between different isotopes or hyperfine components were calibrated by means of a confocal Fabry-Perot interferometer with a free spectral range of 125 MHz. In this way isotope shifts and hyperfine splittings can be determined with a relative accuracy of about  $\pm 10$  MHz.

### III. THEORY

In two-electron systems the *msns* configuration can form two terms, the  $^1S_0$  and  $^3S_1$  states. If the nucleus has no spin ( $I=0$ ) these states are single terms without any hyperfine splitting, and they both converge for a given isotope with increasing principal quantum number  $n$  to the common ionization limit  $I_s$ . In the case of the alkaline earths this is the  $^2S_{1/2}$  ground state of the corresponding ion. If there are no configuration interactions or perturbations of other states these series follow a simple Rydberg formula:

$$E_i = I_s - \frac{R}{(n - \delta_i)^2}, \quad i = 1, 3 \quad (1)$$

where  $\delta_i$  is the quantum defect for singlet and triplet states, respectively, and  $R$  is the Rydberg constant.

With a nuclear spin  $I \neq 0$ , on the other hand, the triplet state is split into  $2J + 1$  hyperfine components for  $I > J$  (or  $2I + 1$  if  $J > I$ ,  $J$  is the total angular momentum of the electrons) with the total angular momenta  $F = |I - J|, |I - J + 1|, \dots, |I + J|$ . The ionization limit is also split into two hyperfine components with  $F = I + \frac{1}{2}$  and  $F = I - \frac{1}{2}$ , and the Rydberg formula (1) does not hold for high principal quantum numbers ( $I_s - E_i \leq$  hyperfine splitting of the ion) when detected with sufficiently high resolution. An additional energy  $\Delta E_i$  has to be added to Eq. (1), which accounts for two different ionization limits.

Using a simple vector model, as shown in Fig. 2, the qualitative behavior can be described easily. For low principal quantum numbers  $n$  the electro-

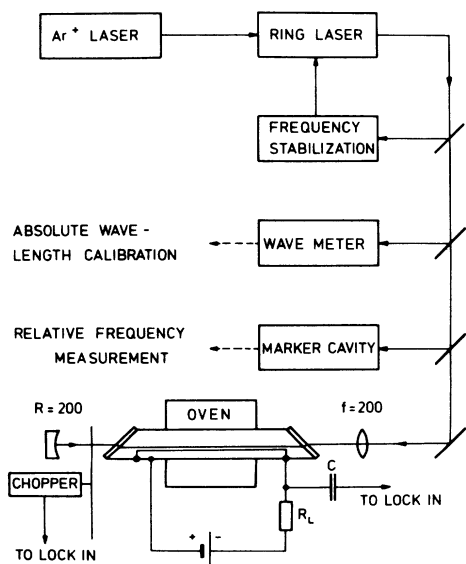


FIG. 1. Scheme of the experimental setup, including the geometry for the Doppler-free two-photon spectroscopy and the detection method.

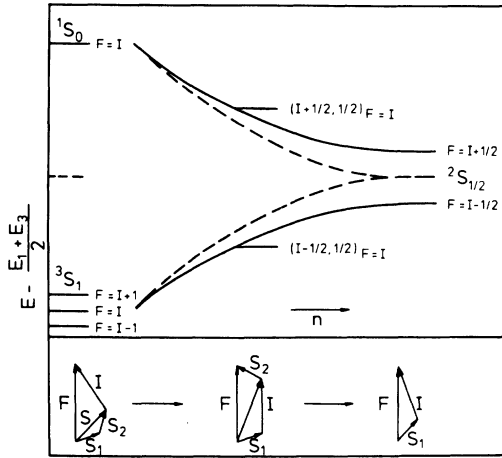


FIG. 2. Change from  $LS$  to  $Is_1$  coupling when approaching the ionization limit. The  $F = \frac{9}{2}$  components of the  ${}^1S_0$  and  ${}^3S_1$  states converge to the  $F = I \pm \frac{1}{2}$  hyperfine components of the ion ground state ( $I \neq 0$ ), whereas for  $I = 0$  all levels merge into the unsplit  ${}^2S_{1/2}$  ionization limit. The energy at the left is not drawn to scale.

static interaction between the two electrons can be regarded as pure Russell-Saunders coupling. This is certainly true in the case of magnesium and calcium and for low  $n$  also for strontium and barium.<sup>9</sup> With increasing principal quantum number, however, the magnetic interaction between the nucleus and the lower  $s$  electron becomes comparable to the spin-spin interaction.<sup>10</sup> This results in a breakdown of pure  $LS$  coupling. The spin of the lower electron now first couples to the nuclear spin to form  $I \pm s_1$  and then couples to the spin of the excited electron to form a total  $F$ . In this  $Is_1$  coupling scheme we still have the same total angular momenta  $F$  as compared to the  $LS$  coupling case. However, when the outer electron becomes ionized, the four states merge into the two hyperfine components of the ion ground state. For a Fermi contact term  $a_{ms} > 0$  the  ${}^1S_0$  state of an isotope with  $I \neq 0$  is higher in energy compared to the  $I = 0$  counterpart which converges to the unsplit  ${}^2S_{1/2}$  state.

The  ${}^3S_1$  ( $F = I$ ) states are lowered in energy, as their ionization limit is the  $F = I - \frac{1}{2}$  hyperfine component. The maximum shift is given by the amount of the hyperfine splitting of the ion ground

state and is directly related to the Fermi contact term of the lower  $s$  electron and the nuclear spin:  $E_{\max}({}^1S_0) = (a_{ms}/2)I$  and  $E_{\max}({}^3S_1) = -(a_{ms}/2)(I+1)$ .<sup>11</sup> The other two components of the  ${}^3S_1$  with  $F = I + 1$  and  $F = I - 1$  converge to the  $I + \frac{1}{2}$  and  $I - \frac{1}{2}$  ion state, respectively. They are not considered in this discussion as only states with the same total angular momentum interact strongly in first order.

A measurement of the isotope shift of  $msns$   ${}^1S_0$  states between even ( $I = 0$ ) and odd ( $I \neq 0$ ) isotopes of alkaline-earth elements as a function of the principal quantum number should clearly show this energy shift for high  $n$ . The energies of the excited states have to be high enough so that the singlet-triplet separation becomes comparable to or smaller than the Fermi contact term, which determines the hyperfine splitting of the ion ground state. In this case the pure  $LS$  coupling breaks down and the  $Is_1$  coupling takes over.

A quantitative calculation of the singlet-triplet shift, which was carried out recently for  ${}^{87}\text{Sr}$ ,<sup>12</sup> is based on the solution of the eigenvalue problem of the perturbed Hamiltonian using mixed wave functions. We will briefly describe the principle of the calculations and then develop a general equation for the hyperfine-induced shift as a function of  $n$  where the nuclear spin is the only parameter. These results can be used to calculate the shift for all odd isotopes of two-electron atoms with a nuclear spin  $\frac{3}{2} \leq I \leq \frac{9}{2}$ , provided the singlet-triplet splitting is known.

The Hamiltonian  $H_0$  of the unperturbed system has to be extended by the Fermi contact term<sup>11</sup>

$$W = \text{const } \vec{I} \cdot \vec{s} . \quad (2)$$

The wave function  $|\Psi\rangle$  is taken as a linear combination of the singlet and triplet wave functions with the total angular momentum  $F = I$ :

$$|\Psi\rangle = a_1 |\Psi_1(F=I)\rangle + a_3 |\Psi_3(F=I)\rangle . \quad (3)$$

Diagonalization of  $H$  and considering that

$$H_0 |\Psi_1\rangle = E_1 |\Psi_1\rangle$$

and

$$H_0 |\Psi_3\rangle = E_3 |\Psi_3\rangle$$

results in the following secular equation for the perturbed eigenvalues  $\tilde{E}$  of  $H$ :

$$\det \begin{vmatrix} E_1 + \langle \Psi_1 | W | \Psi_1 \rangle - \tilde{E} & \langle \Psi_1 | W | \Psi_3 \rangle \\ \langle \Psi_3 | W | \Psi_1 \rangle & E_3 + \langle \Psi_3 | W | \Psi_3 \rangle - \tilde{E} \end{vmatrix} = 0 . \quad (5)$$

The matrix elements are given by<sup>13</sup>

$$\begin{aligned} \langle \Psi_1 | W | \Psi_1 \rangle &= 0, & \langle \Psi_1 | W | \Psi_3 \rangle &= \frac{a_{ms}}{2} [I(I+1)]^{1/2}, \\ \langle \Psi_3 | W | \Psi_3 \rangle &= -\frac{a_{ms}}{2}, & \langle \Psi_3 | W | \Psi_1 \rangle &= \frac{a_{ms}}{2} [I(I+1)]^{1/2}. \end{aligned} \quad (6)$$

From (5) and (6) it follows that

$$\tilde{E}_{1/3} = \frac{E_1 + E_3}{2} - \frac{a_{ms}}{4} \pm \frac{1}{2} [(E_1 - E_3)^2 + a_{ms}(E_1 - E_3) + a_{ms}^2(I + \frac{1}{2})^2]^{1/2}. \quad (7)$$

The energy differences  $\Delta E_{1/3}$  to the unperturbed term values  $E_1$  and  $E_3$  due to the hyperfine interaction are then given by

$$\begin{aligned} \Delta E_1 = \tilde{E}_1 - E_1 &= -\frac{E_1 - E_3}{2} - \frac{a_{ms}}{4} + \frac{1}{2} [(E_1 - E_3)^2 + a_{ms}(E_1 - E_3) + a_{ms}^2(I + \frac{1}{2})^2]^{1/2}, \\ \Delta E_3 = \tilde{E}_3 - E_3 &= \frac{E_1 - E_3}{2} - \frac{a_{ms}}{4} - \frac{1}{2} [(E_1 - E_3)^2 + a_{ms}(E_1 - E_3) + a_{ms}^2(I + \frac{1}{2})^2]^{1/2}. \end{aligned} \quad (8)$$

It is more convenient to express the energies in units of the Fermi contact term  $a_{ms}$ . Equations (8) then read

$$\eta_{1/3}^+ = \mp \frac{1}{2} \xi - \frac{1}{4} \pm \frac{1}{2} [\xi^2 + (I + \frac{1}{2})^2]^{1/2}, \quad (9)$$

with  $\eta_{1/3} = (\tilde{E}_{1/3} - E_{1/3})/a_{ms}$ . Equation (9) holds only for positive  $a_{ms}$  as indicated by the superscript  $+$ . If the Fermi contact term is negative, the hyperfine components of the ion ground state are reversed and the two  $F=I$  states of  $^1S_0$  and  $^3S_1$  are supposed to cross. But as both states have the same total angular momentum  $F$  they repel each other and the  $^1S_0$  ( $F=I$ ) state merges into the  $F=I - \frac{1}{2}$  ion component and the  $^3S_1$  ( $F=I$ ) states end in the  $F=I + \frac{1}{2}$  hyperfine state. In the simple vector model this case can be accounted for by changing the quantum numbers in  $Is_1$  coupling. The ordering of the hyperfine components of the  $^3S_1$  state is in this case also reversed.

For  $a_{ms} < 0$  Eq. (9) has to be replaced by

$$\eta_{1/3}^- = \mp \frac{1}{2} \xi - \frac{1}{4} \mp \frac{1}{2} [\xi^2 + \xi + (I + \frac{1}{2})^2]^{1/2}. \quad (10)$$

Figure 3 shows  $\eta_{1/3}^+$  for different values of  $I$ . The graph can be used to determine the hyperfine-induced shift for all alkaline-earth elements with different nuclear spins and both positive and negative  $a_{ms}$ . Let us discuss briefly some characteristic

features. The energy shift of the  $^3S_1$  ( $F=I$ ) series converges both for  $a_{ms} < 0$  and  $a_{ms} > 0$ , with  $|\xi| \rightarrow \infty$ ,  $[(E_1 - E_3) \gg a_{ms}]$  to the limit

$$(\eta_3^+)_{\infty} = (\eta_3^-)_{\infty} = -\frac{1}{2} \quad (11)$$

or

$$\Delta E_3^+ = -\frac{a_{ms}}{2},$$

which is the hyperfine splitting of the  $^3S_1$  ( $F=I$ ) state without any perturbations. This is the case for large singlet-triplet separations at low principal quantum numbers  $n$ . In the high- $n$  limit with small singlet-triplet energy differences ( $|\xi| \rightarrow 0$ ) it follows that

$$(\eta_3^+)_{0} = -\frac{1}{2}(I+1) \quad (12)$$

or

$$\Delta E_3^+ = -\frac{a_{ms}}{2}(I+1),$$

and

$$(\eta_3^-)_{0} = \frac{1}{2}I \quad (13)$$

or

$$\Delta E_3^- = \frac{a_{ms}}{2}I.$$

Hence for different signs of  $a_{ms}$  the  $^3S_1$  ( $F=I$ ) series converge with increasing principal quantum numbers  $n$  to different hyperfine states of the ion.

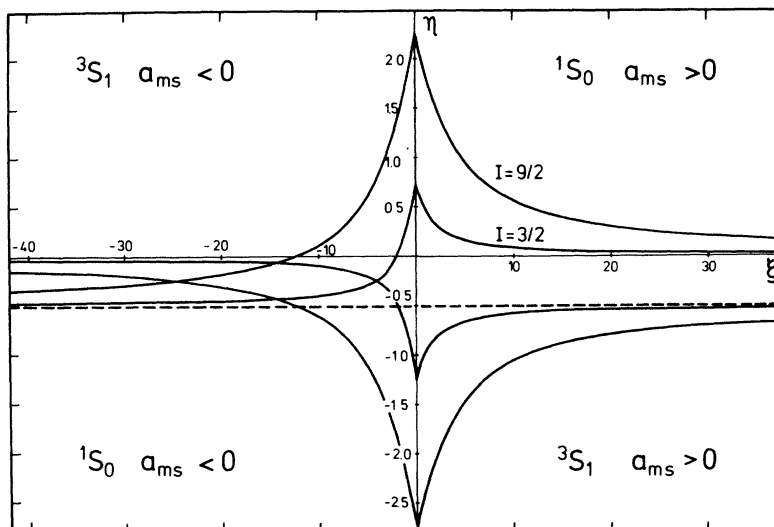


FIG. 3. Calculated level shifts for the  $F = \frac{9}{2}$  components of  $^1S_0$  and  $^3S_1$  for different nuclear spins as a function of singlet-triplet separation. The energy shift and the singlet-triplet separation are normalized to the Fermi contact term  $a_{ms}$ . For further details see text.

The  $^3S_1$  ( $F=I$ ) series always ends in the lower component of the hyperfine doublet.

The energy shift of the  $^1S_0$  ( $F=I$ ) series converges to zero for  $|\xi| \rightarrow \infty$  as expected. For small  $|\xi|$  we have again two different limits for  $\eta_1^+$  and  $\eta_1^-$ , due to the reversal of hyperfine splitting of the ion ground state. These limits are

$$\eta_1^+ = \frac{1}{2}I$$

or

$$\Delta E_1^+ = \frac{a_{ms}}{2}I, \quad (14)$$

$$\eta_1^- = -\frac{1}{2}(I+1)$$

or

$$\Delta E_1^- = -\frac{a_{ms}}{2}(I+1). \quad (15)$$

It is obvious that the amount of the energy shift is proportional both to the nuclear spin and the Fermi contact term. Hence even isotopes with  $I=0$  are not shifted even if their wave functions are strongly mixed.

#### IV. RESULTS AND DISCUSSION

##### A. Strontium

Strontium is a very favorable case for the observation of the hyperfine-induced level shift. It has

three stable even isotopes ( $^{84}\text{Sr}$ : 0.56%,  $^{86}\text{Sr}$ : 9.86%, and  $^{88}\text{Sr}$ : 82.56% isotopic abundance in the natural admixture) with the nuclear spin  $I=0$  and one odd isotope ( $^{87}\text{Sr}$ : 7.02%) with  $I = \frac{9}{2}$ . The maximum shift is rather large (2.75 GHz) so that even at low principal quantum numbers a pronounced energy shift can be observed. On the other hand, the transition probability for two-photon transitions is enhanced due to a suitable intermediate level: the  $5s\ 5p\ ^1P_1$  resonance level at  $21\ 698.48\ \text{cm}^{-1}$ . Therefore also states with high principal quantum numbers can be excited. In addition, the output power of the Stilbene 3 dye laser peaks at 435 nm corresponding to a two-photon energy of  $45\ 977\ \text{cm}^{-1}$ . Rydberg states with a principal quantum number  $n=9$  up to the ionization limit are accessible with this dye. The term energies up to  $n=36$  were taken from the work of Rubbmark.<sup>14</sup> For higher- $n$  values the positions of the states were calculated using Eq. (1).

Typical spectra of different  $msns\ ^1S_0$  Rydberg states of Sr as obtained with two-photon excitation are shown in Fig. 4. All stable Sr isotopes are resolved. The isotope shifts between even isotopes are dominated by the normal mass shift. As they all have the nuclear spin  $I=0$  there is no additional energy shift due to hyperfine interactions. However, the energy shift of the odd  $^{87}\text{Sr}$  isotope depending on the principal quantum number as discussed above can be observed clearly. In order to exclude other effects which also can shift the term energies, various parameters were changed

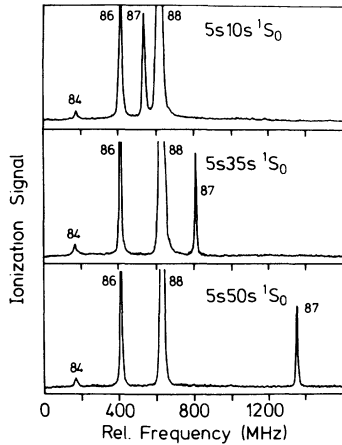


FIG. 4. Doppler-free two-photon excitation spectra from the  $5s^2 1S_0$  ground state to different  $5sns 1S_0$  Rydberg states. The isotopes are labeled by their mass numbers.

during the experiment. Different voltages across the pipe ( $0.1 \text{ V} < U < 10 \text{ V}$ ) and external magnetic fields up to several hundred gauss did not influence the relative positions of the isotopes within our accuracy. The isotope shifts also remained unaffected if the Sr vapor pressure was varied or if a buffer gas (He, Ne) was added. A contribution of the ac Stark effect was negligible as verified by changing the laser power by a factor of 5.

The comparison between experimentally obtained level shifts of the odd isotope and calculated values using Eq. (10) is shown in Fig. 5. The experimental data were determined by measuring the isotope shift between  $^{86}\text{Sr}$  and  $^{87}\text{Sr}$  and subtracting the normal mass shift. The remaining shift represents a combination of the hyperfine-induced level shift, the specific mass shift, and the field shift. The

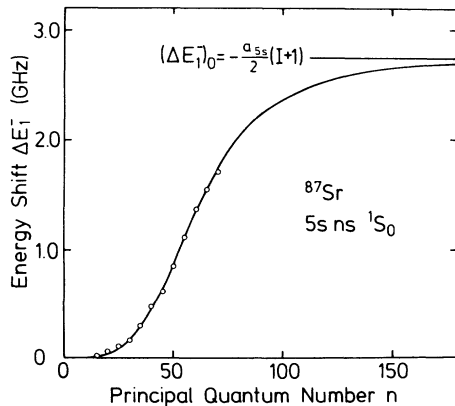


FIG. 5. Calculated energy shift for  $^{87}\text{Sr}$  as a function of the principal quantum number  $n$ . Circles represent the experimental data.

latter two should show no  $n$ -dependence and are neglected for Sr.<sup>6</sup> The theoretical curve was calculated taking the Fermi contact term  $a_{5s} = -0.99 \text{ GHz}$ .<sup>15</sup> The singlet-triplet energy differences as a function of  $n$  were derived using Eq. (1) and the following parameters:  $I_s = 45932.19 \text{ cm}^{-1}$ ,<sup>16</sup>  $\delta_1 = 3.269$ ,<sup>16</sup>  $\delta_3 = 3.37$ .<sup>17</sup> At low principal quantum numbers ( $n < 30$ ) there is only a small increase of the energy shift, above  $n \sim 30$  the shift increases drastically and finally starts to saturate at  $n \sim 80$ , converging to the  $F = I - \frac{1}{2}$  hyperfine component of the Sr II  $^2S_{1/2}$  ground state with a maximum shift of 2.75 GHz. There is excellent agreement between theory and experiment.

## B. Calcium

The natural mixture of calcium contains one stable odd isotope,  $^{43}\text{Ca}$  ( $I = \frac{7}{2}$ ), with an abundance of only 0.135 at. %. Figure 6 shows a laser scan over the  $4s 10s 1S_0$  Rydberg state with the well resolved  $^{43}\text{Ca}$  and the even isotopes  $^{40}\text{Ca}$  (96.97 at. %),  $^{42}\text{Ca}$  (0.64 at. %),  $^{44}\text{Ca}$  (2.06 at. %), and  $^{48}\text{Ca}$  (0.185 at. %) demonstrating the high detection sensitivity of the space-charge limited thermionic diode. However, the two-photon transition probabilities for the  $4sns 1S_0$  series decrease drastically above  $n \sim 15$  with increasing quantum number as already observed by Wynne *et al.*<sup>18</sup> Thus in the case of calcium the isotope  $^{43}\text{Ca}$  could only be detected up to  $n = 21$  at a corresponding laser wavelength of 408.2 nm. Here, the single-mode output power of the ring laser working with Stilbene 1 was limited to about 30 mW only. In comparison, the hyperfine components of the  $4snd 1D_2$  levels have been resolved up to  $n = 50$  (laser wavelength  $\sim 406 \text{ nm}$ ) with the same experimental setup.<sup>19</sup> When employing time averaging

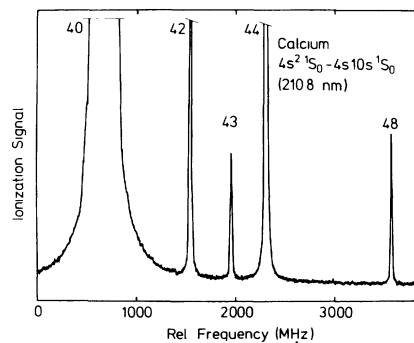


FIG. 6. Two-photon excitation spectrum for the  $4s^2 1S_0 - 4s 10s 1S_0$  transition in natural calcium.

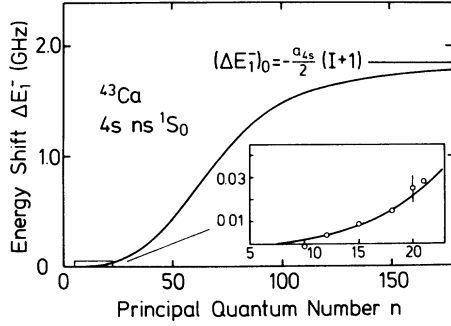


FIG. 7. Calculated energy shift for  $^{43}\text{Ca}$  as a function of the principal quantum number  $n$ . In the insert experimental data are compared with the prediction. The error bar represents the error intervals for all determined data.

using a frequency offset locking system<sup>20</sup> it should be possible to record data also for high  $ns\ ^1S_0$  levels of  $^{43}\text{Ca}$ . Work along this line is in progress.

Figure 7 shows the theoretical level shift for  $^{43}\text{Ca}$  using again Eqs. (1) and (10) with the following parameters:  $I = \frac{7}{2}$ ,  $I_s = 49\,305.99\ \text{cm}^{-1}$ ,  $\delta_1 = 2.337$  (Ref. 18), and  $\delta_3 = 2.441$ .<sup>21</sup> The Fermi contact term  $a_{4s}$  was calculated with the Fermi-Segré-Goudsmit formula<sup>22</sup> to  $a_{4s} = -0.827\ \text{GHz}$ . In the insert the experimental data are compared with theory, showing reasonable agreement. The experimental values were obtained applying the same procedure as for strontium. The contribution of specific mass and field shift is reduced by normalization of the data for  $n = 12$  to the theoretical value. Although we did not measure very high- $n$  values the trend for the odd-even energy shift is obvious.

### C. Barium

The natural isotopic mixture of barium is composed of five even and two odd isotopes, both with the nuclear spin  $I = \frac{3}{2}$ . The energy shifts of  $^{135}\text{Ba}$  (6.59%) and  $^{137}\text{Ba}$  (11.32%)  $6sns\ ^1S_0$  states were analyzed between the principal quantum numbers  $n = 21$  ( $41\,646.38\ \text{cm}^{-1}$ ) and  $n = 50$  ( $41\,982.68\ \text{cm}^{-1}$ ) with respect to  $^{138}\text{Ba}$  (71.66%).

The  $a_{6s}$  factors of  $\text{Ba}^+$  are known very accurately<sup>23</sup>:  $a_{6s}(^{135}\text{Ba}^+) = 3.591\,67\ \text{GHz}$  and  $a_{6s}(^{137}\text{Ba}^+) = 4.018\,87\ \text{GHz}$ . While the nuclear spins of both isotopes are identical, a slightly larger increase of the energy shift for  $^{137}\text{Ba}$  should be obtained due to the larger value of  $a_{6s}$  for  $^{137}\text{Ba}$  compared to  $^{135}\text{Ba}$ .

The energy difference ( $E_1 - E_3$ ), which is necessary for the calculations, cannot be extracted from the literature, because  $6sns\ ^3S_1$  levels are not known for values  $n \geq 12$ . The known term values are of little use, however, since in these lower regions of the principal quantum numbers perturbations affect the term energies considerably.

To obtain a reasonable value for the quantum defect  $\delta_3$  we took our experimentally derived energy shift for  $n = 50$  and the known  $\delta_1$  for the singlet series to determine the quantum defect for high values of  $n$  for the  $6sns\ ^3S_1$  levels of barium. At this point it should be mentioned that the theory presented above also offers the possibility to determine exact term energies for Rydberg series, which are not easily accessible for experimental investigations due to selection rules, provided the wave function does not contain contributions from other configurations.

With the data for the quantum defect derived in this way [ $\delta_1 = 4.218$  (Ref. 24) and  $\delta_3 = 4.280$ ], taking the revised ionization limit for barium  $42\,035.04\ \text{cm}^{-1}$  (Ref. 24) and subtracting again the normal mass shift for the isotope shifts  $^{138}\text{Ba} - ^{137}\text{Ba}$  and  $^{138}\text{Ba} - ^{135}\text{Ba}$ , the comparison between experiment and theory is illustrated in Fig. 8 for both odd Ba isotopes. Again, the experimental data closely follow the theoretical predictions. The larger increase for  $^{137}\text{Ba}$  is verified by the experiment. Deviations from the calculation for low  $n$  are mainly due to the influence of perturbing states such as  $6p\ ^2\ ^3P_0$ ,  $5d\ 6d\ ^3D_0$ , and  $5d\ 6d\ ^1S_0$ .<sup>24</sup> Specific mass and volume shifts are considerably affected by these perturbations.

In addition, there are many more interacting lev-

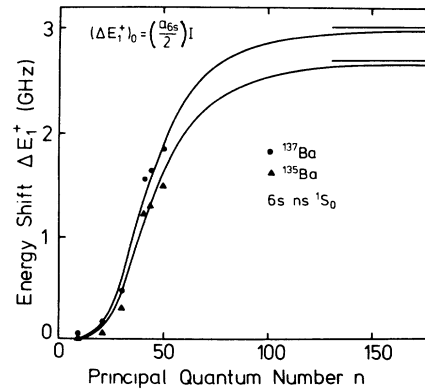


FIG. 8. Calculated energy shifts for  $^{135}\text{Ba}$  and  $^{137}\text{Ba}$  as a function of the principal quantum number  $n$ . Experimental data for  $^{135}\text{Ba}$  and  $^{137}\text{Ba}$  are added for comparison. The values for  $n = 9$  were taken from Ref. 26.

els in the barium spectrum also for high principal quantum numbers  $n$  as can be seen from the work of Aymar *et al.*<sup>24</sup> These perturbations can lead to slightly different energy shifts, because they are not included in this simple theory.

## V. SUMMARY

In conclusion, we have demonstrated that high-resolution two-photon spectroscopy of alkaline-earth elements in high Rydberg states can gain accurate information about singlet-triplet mixing induced by hyperfine interactions. The effect of the energy shift first observed for the odd <sup>87</sup>Sr isotope occurs also in other alkaline-earth elements, as was demonstrated by the data for <sup>43</sup>Ca, <sup>135</sup>Ba, and <sup>137</sup>Ba. These data are compared with calculated values taking into account the interactions of  $F=I$  hyperfine levels of <sup>1</sup>S<sub>0</sub> and <sup>3</sup>S<sub>1</sub> states only. There is good agreement between experiment and theory, although the influence of  $F=I$  hyperfine states of <sup>1</sup>D<sub>2</sub>, <sup>3</sup>D<sub>1,2,3</sub>, or other series are neglected. The theory allows for the determination of term ener-

gies or quantum defects even for levels which are not accessible to experimental analysis due to vanishing transition probabilities.

Similar behavior is expected for <sup>1</sup>D<sub>2</sub> and <sup>3</sup>D<sub>2</sub>, which was observed<sup>25</sup> for the same isotopes discussed here; this effect requires an extended theory due to additional terms necessary in the Hamiltonian and more interacting levels involved.

In principle, the observed shifts have to be taken into account for all isotopes with nuclear spin  $I \neq 0$ , when term energies of Rydberg states are determined with very high accuracy and multichannel quantum defect theory (MQDT) is applied.

## ACKNOWLEDGMENTS

The authors gratefully acknowledge stimulating discussions with Professor E. Matthias. We also wish to thank Dr. H. Klar and Dr. R. Wallenstein for their interest in this work and for valuable contributions. This work was supported by the Deutsche Forschungsgemeinschaft, Sfb 161.

- 
- <sup>1</sup>P. F. Liao, R. R. Freeman, R. Panock, and L. M. Humphrey, *Opt. Commun.* **34**, 195 (1980).  
<sup>2</sup>F. Biraben, E. de Clerq, E. Giacobino, and G. Grynberg, *J. Phys. B* **13**, L685 (1980).  
<sup>3</sup>R. R. Freeman, P. F. Liao, R. Panock, and L. M. Humphrey, *Phys. Rev. A* **22**, 1510 (1980).  
<sup>4</sup>E. de Clerq, F. Biraben, E. Giacobino, G. Grynberg, and J. Bauche, *J. Phys. B* **14**, L183 (1981).  
<sup>5</sup>R. Beigang, E. Matthias, and A. Timmermann, *Phys. Rev. Lett.* **47**, 326 (1981).  
<sup>6</sup>R. Beigang, E. Matthias, and A. Timmermann, *Z. Phys.* **A301**, 93 (1981).  
<sup>7</sup>See, for example, G. Grynberg and B. Cagnac, *Rep. Prog. Phys.* **40**, 791 (1977) and references therein.  
<sup>8</sup>P. Esherick and J. J. Wynne, *Comments Mol. Phys.* **1**, 43 (1977) and references therein.  
<sup>9</sup>J. J. Wynne and J. A. Armstrong, *IBM J. Res. Dev.* **23**, 490 (1979).  
<sup>10</sup>S. Goudsmit and R. F. Bacher, *Phys. Rev.* **34**, 1501 (1929).  
<sup>11</sup>H. Kopfermann, *Nuclear Moments* (Academic, New York, 1958).  
<sup>12</sup>H. Rinneberg, *Z. Phys.* **A302**, 363 (1981).  
<sup>13</sup>A. Lurio, M. Mandel, and R. Novick, *Phys. Rev.* **126**, 1758 (1962).  
<sup>14</sup>J. R. Rubbmark and S. A. Borgström, *Phys. Scr.* **18**, 196 (1977).  
<sup>15</sup>M. Heyden and H. Kopfermann, *Z. Phys.* **108**, 232 (1938).  
<sup>16</sup>P. Esherick, *Phys. Rev. A* **15**, 1920 (1977).  
<sup>17</sup>K. C. Pandey, S. Jha Sudhanshu, and J. A. Armstrong, *Phys. Rev. Lett.* **44**, 1583 (1980).  
<sup>18</sup>See, for example, J. A. Armstrong, P. Esherick, and J. J. Wynne, *Phys. Rev. A* **15**, 180 (1977).  
<sup>19</sup>R. Beigang, K. Lücke, E. Matthias, and A. Timmermann (unpublished).  
<sup>20</sup>H. Gerhardt, F. Jeschonnek, W. Makat, F. Schneider, A. Timmermann, R. Wenz, and P. J. West, *Appl. Phys.* **22**, 361 (1980).  
<sup>21</sup>C. E. Moore, *Atomic Energy Levels*, Natl. Bur. Stds. (U. S.) Circ. No. 467 (U. S. GPO, Washington, D. C., 1957).  
<sup>22</sup>I. I. Sobelman, *Atomic Spectra and Radiative Transitions* (Springer, Berlin, 1979).  
<sup>23</sup>F. v. Sichart, H. J. Stöckermann, H. Ackermann, and G. zu Putlitz, *Z. Phys.* **236**, 97 (1970).  
<sup>24</sup>M. Aymar, P. Camus, M. Dieulin, and C. Morillon, *Phys. Rev. A* **18**, 2173 (1978).  
<sup>25</sup>R. Beigang, E. Matthias, A. Timmermann, and P. West (unpublished).  
<sup>26</sup>W. Jitschin and G. Meisel, *Z. Phys.* **A295**, 37 (1980).